IEEE Sensors Council

Force Sensor Based on FBG Embedded in Silicone Rubber

Pasquale Di Palma, Elena De Vita, *Member, IEEE*, Agostino Iadicicco, *Member, IEEE*, and Stefania Campopiano, *Member, IEEE*

***Abstract*—Force sensing is a key enabler for getting haptic feedback, useful in a variety of applications, especially in the fields of robotics, automation, and health. Indeed, equipping machines, vehicles, robots, and even humans with force sensors provides controlled processes and production, safe and enhanced external interaction, and capability to perform efficient manipulation and precise movements. Aiming to develop an alternative solution to electrical force sensors, in this work a fiber Bragg grating (FBG) is embedded inside a patch made of silicone rubber. Such embedding strategy allows to make the FBG sensitive to the force variations, obtain a flexible patch having a moldable shape, and protect the most fragile areas of the optical fiber. Moreover, due to its high flexibility and stretchability, the sensing patch can be easily employed as portable and wearable device. Besides reporting fabrication process and results of the performed force tests, this work provides a systematic study of the FBG embedding in a silicone matrix. Indeed, for this purpose, three sensing patches having different thicknesses are developed and tested in temperature, strain, and force, finding that the patch thickness influences the sensing performances of the device. The resulting force sensitivity varies in the range from 9.2 to 19.0 pm/N, based on the sensor thickness. Temperature sensitivity, instead, is comparable with respect to bare FBGs, while strain sensitivity is enormously reduced, obtaining a patch able to insulate the FBG from the strain variations.**

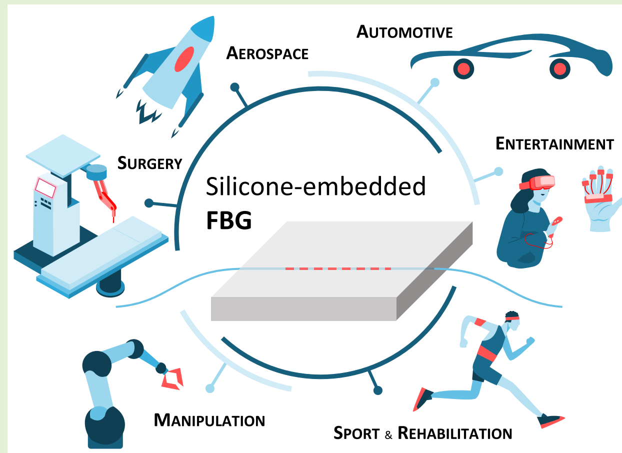

***Index Terms*—Fiber Bragg grating (FBG) embedding, FBGs, fiber optic sensors, force sensing, haptic feedback, silicone.**

I. Introduction

FORCE sensors transduce transversal force in an electromagnetic signal and are essential in a variety of fields spanning from industrial production and processing to sport and medical applications, including automotive, aeronautical, entertainment, collaborative, rehabilitative, and surgical robotics. In all these fields, indeed, accurate manipulation is crucial, requiring the capability of performing challenging tasks and fine movements with high precision and coordination. Moreover, in robotics applications, the interaction between humans and machines plays a pivotal role both when the contact with the robot components can be detrimental to humans (i.e., industrial robots) and when the machine is designed to interact with the human body, as in the case of surgical or collaborative robots (i.e., cobots). Either way, protection, risk mitigation, and environmental adaptation are the key words for a safe and functional coexistence of both men and robots also in constrained spaces [1]. In this scenario, force sensing becomes the solution to provide haptic feedback for a controlled human–machine interactions, able to accomplish an efficient and reliable manipulation.

The most studied and widely employed measurement instruments for force sensing purposes are based on piezoelectric, magnetic, inductive, capacitive methods, and, from the early 1980s, fiber optic sensors [2]. In particular, commercially available force sensors rely on strain gauges and microelectromechanical systems (MEMS) [3]. Although they offer low manufacturing costs and a proven technology, such sensors introduce two major drawbacks, lying in their electrical nature and lack of flexibility, given by the brittleness of their components [4]. These disadvantageous aspects represent a crucial point especially considering the dramatically growing interest in soft robotics, smart prosthetics, and wearable sensors [5], [6], toward measuring systems increasingly focused on

Manuscript received 11 October 2022; revised 17 November 2022; accepted 17 November 2022. Date of publication 6 December 2022; date of current version 12 January 2023. The associate editor coordinating the review of this article and approving it for publication was Prof. Carlos Marques. *(Corresponding author: Elena De Vita.)*

The authors are with the Dipartimento di Ingegneria, Università degli Studi di Napoli Parthenope, 80143 Naples, Italy (e-mail: elena.devita001@studenti.uniparthenope.it).

Digital Object Identifier 10.1109/JSEN.2022.3226039

the easy interaction with human body, long-term monitoring, and operational safety for the users. In this respect, in recent years, wearable electronic devices based on flexible materials have gained momentum, enhancing the compliance between humans and robots.

Fiber optic-based systems represent a safer alternative since the absence of electric currents and connections and thus their intrinsic immunity to electromagnetic interferences. Such characteristic, together with the great high-temperature performances, makes fiber optics extremely environmentally resistant sensors. Moreover, such devices offer multiplexing capabilities and very compact size, which enable not only the miniaturization of the sensing system while maximizing the sensing points but also the possibility to embed the sensor inside elements of various nature and composition [7]. Among fiber optic sensors, fiber Bragg gratings (FBGs) rely on wavelength modulation, overcoming the typically limited accuracy and repeatability of the light intensity modulated sensors, which indeed are susceptible to the effects of fluctuation in input light intensity and fiber bending loss [8].

In the literature, several strategies and materials have been implemented to develop force sensors based on the FBG technology. Hu et al. [9] reported about a surface sticking method to obtain a force sensor based on two FBGs and a substrate having two strain bodies (i.e., positive and negative) adhered to the surface able to detect force increments with a sensitivity of 38.25 pm/kN. Song et al. [10] developed a force sensing tool for minimally invasive robotic surgery based on a load cell consisting of eight FBGs to measure the force applied on the tool tip, where half of the sensors are employed only for temperature compensation. Müller et al. [11], instead, proposed to paste an array of six FBGs on a polymeric structure able to perform force–torque measurements for laparoscopic instruments. However, such techniques of FBG bonding for force detection offer limited sensitivities and the risk of chirping failure due to the nonuniform strain distribution [12]. Shi et al. [13] tried to overcome this limitation by implementing a suspended fiber configuration, i.e., by bonding only two points of the fiber to the flexure in correspondence of two carved grooves, rather than gluing the whole fiber. The structure of the proposed device is based on the Stewart platform, a suspended FBG sensor, and a contact head, enabling force measurements with a sensitivity up to 21 mN. Despite the force sensitivity increase, it is worth noting that such strategies, due to both the employed materials and the size of the developed sensors, do not provide either flexible or wearable device.

For these reasons, embedding of FBGs in soft compounds represents the turning point for force sensing toward wearability and flexibility. Wang et al. [14] described an FBG packaging technique to obtain a force sensor for a medical application (i.e., the graduated compression bandaging of the lower limbs). They incorporate the FBG sensor into a flat and flexible tape and the collected force measurements, calibrated to be expressed as contact pressure, and exhibit a sensitivity of about 4.8 pm/mmHg. Leal-Junior et al. [15], instead, proposed a thermoplastic polyurethane flexible structure to embed an array of two FBGs inscribed in cyclic, transparent, optical polymer (CYTOP) in such a way as to assess the exchanged forces with a lower limb exoskeleton for knee rehabilitation. In [16] and [17], they also report about the development of a polymeric optical fiber (POF) strain gauge, based on the power attenuation due to the misalignment between two POFs, and the FBG embedding inside 3-D printed patches made of acrylonitrile butadiene styrene (ABS). While the first device cannot provide the multiplexing capabilities of FBGs, but shows temperature insensitivity, the second one exploits the typical advantages of FBGs, revealing a strong dependence of its temperature and force sensitivities on the infill density of the 3-D printed material. However, in the literature, it is pointed out that an excellent degree of flexibility can be obtained by employing silicone elastomers and natural rubbers as substrate materials for FBGs embedding. Embedding procedures based on such materials enables flexible sensors of various parameters, i.e., curvature, respiratory and cardiac rate, joint movement, weight, and force, as reported in [18], [19], [20], [21], [22], [23], and [24]. All these works describe the working principle of the developed devices and the investigated application of such devices in a certain field.

This article is devoted to address the silicone embedding technique of FBGs for force measurements with a new level of depth, i.e., to propose a systematic study of the performances exhibited by silicone embedded FBGs as a function of different parameters. For this purpose, a flexible patch embedding an FBG and made of silicone rubber is developed. Once detailed the steps that lead to the fabrication of the sensing device, the latter is characterized by varying temperature, force, and strain conditions. Moreover, the sensor behavior as a function of its geometrical features is analyzed, finding out that thickness affects its sensitivity.

The developed device responds to the need for safety and easy human interaction of force sensing, being highly flexible, stretchable, soft, and due to the possibility to be worn and to mold its shape. Silicone embedding proves to protect the most fragile areas of the FBG and to turn it sensitive to the applied force variations.

II. Materials and Method

In this section, the working principle of the sensing element, i.e., the FBG, is detailed. Then, the fabrication process of the developed force sensor is illustrated, highlighting that three devices having different thicknesses are manufactured aiming to compare their sensing performances.

A. FBG Working Principle

An FBG can be obtained by perturbing in a periodical manner the effective refractive index of the core of an optical fiber. The sensing principle on an FBG relies on its filtering behavior: when a broadband light spectrum is injected into the fiber core, the FBG reflects a narrow portion of such spectrum, centered around a wavelength that is specific for the grating and is called Bragg wavelength, i.e., λ_B. Fig. 1 reports the schematic of the working principle of an FBG, with a zoomed-in view correspondence of the grating.

The expression of λ_B is reported in the following equation [25]:

$$\lambda_B = 2 \cdot \Lambda \cdot n_{eff} \tag{1}$$

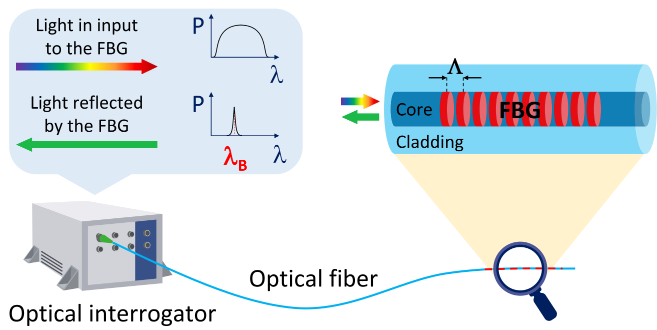

Fig. 1. Working principle of an FBG, with a zoom on the periodic perturbation of the effective refractive index inside the core of the optical fiber.

where Λ is the period of the perturbation, i.e., of the FBG, and n_{eff} is the effective refractive index of the core.

According to (1), the main feature of the FBG, i.e., its λ_{B}, depends on Λ and n_{eff} in such a way as to variations of these parameters induce a shift in λ_{B}, denoted by $\Delta\lambda_{\mathrm{B}}$. Since both Λ and n_{eff} are influenced by variations of the temperature T around the fiber and the strain ε acting on the fiber, FBGs are intrinsically temperature and strain sensors.

The expression of such shift $\Delta\lambda_{\mathrm{B}}$ is the following:

$$\Delta\lambda_{\mathrm{B}} = \frac{\partial\lambda_{\mathrm{B}}}{\partial T}\Delta T + \frac{\partial\lambda_{\mathrm{B}}}{\partial\varepsilon}\Delta\varepsilon = S_T\Delta T + S_\varepsilon\Delta\varepsilon \quad (2)$$

and, thus, it is a function of two coefficients, i.e., thermal sensitivity S_T and strain sensitivity S_ε of the grating, whose values are typically around 10 pm·°C^{-1} and 1.2 pm·$\mu\varepsilon^{-1}$, respectively, for a bare FBG [26].

It is worth noting that, since FBGs are sensitive to T and ε simultaneously, to relate the shift $\Delta\lambda_B$ to only one parameter also when both are varying, two FBGs are needed. In this way, indeed, one sensor is employed in a strain-free configuration and can monitor the sole temperature variations, while the other one monitors the strain variations. Therefore, for the strain characterizations reported in Section III, two FBGs are involved in order to provide both temperature and strain reference.

B. Force Sensor Fabrication

This section reports the fabrication process of the sensing device, lying in a silicone patch embedding the FBG. To analyze the impact of the patch thickness on its sensing properties, three devices with varying thickness and denoted by DS-A, DS-B, and DS-C are fabricated, as reported in the following. The FBG used for these tests is produced by AtGrating Technologies by employing the phase mask method. The optical characteristics of such sensors are reported as follows.

1) $\lambda_{\mathrm{B,A}} = 1534.124$ nm, $\lambda_{\mathrm{B,B}} = 1521.250$ nm, and $\lambda_{\mathrm{B,C}} = 1522.115$ nm, for FBGs embedded DS-A, DS-B, and DS-C patches, respectively.
2) The length of 10 mm for all the involved FBGs.
3) The reflectivity of about 95%.

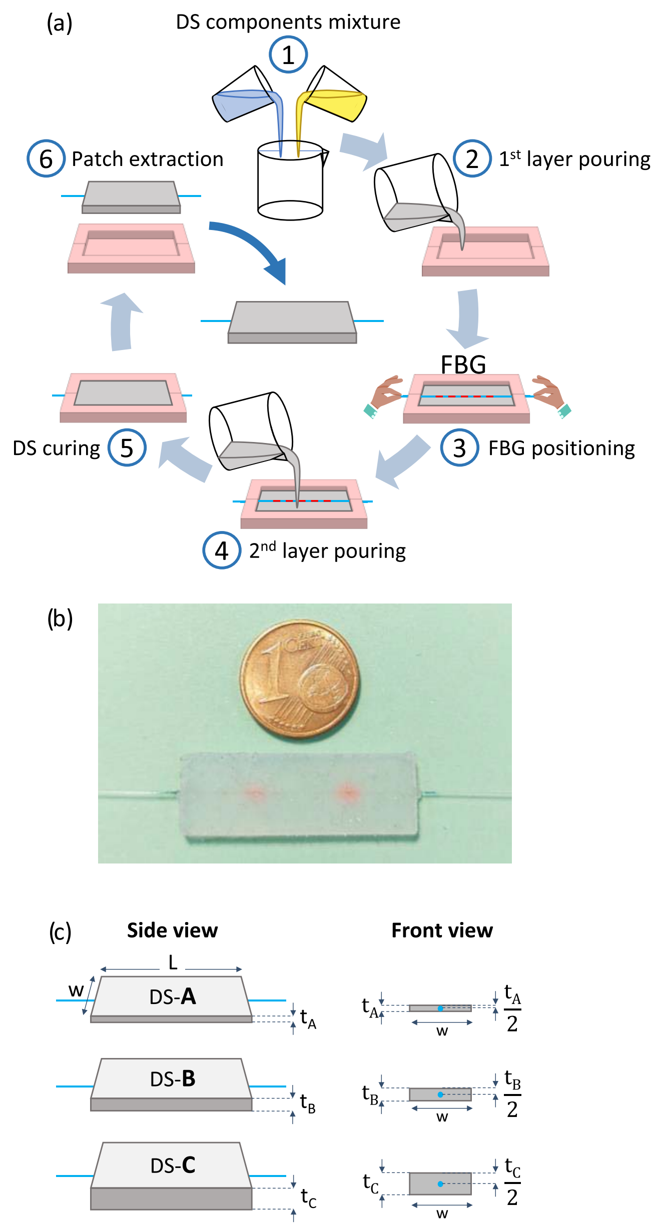

Fig. 2. (a) Fabrication stages of the sensor, (b) photograph of a fabricated sensor (the red spots indicate the FBG position), and (c) schematics of the three developed patches DS-A, DS-B, and DS-C, having different thickness.

The fabrication process consists in the embedding of an FBG in a silicone matrix. More specifically, Dragon Skin[1] (DS) 10 Medium is used since its advantageous features, such as the wide range of operating temperatures, i.e., from −53 °C to 232 °C, the ease of use (indeed, this rubber is simply based on two liquid components and is able to cure at room temperature), and the compatibility with the skin.

Fabrication steps are outlined in Fig. 2(a). The first stage involves the blending of same volumes of the DS liquid parts; 3 min of blending while thoroughly scraping the sides and bottom of the mixing container are enough for obtaining the definitive mixture, which results still liquid but denser. In the

[1]Traditional trademark.

second step, half blend is poured in a 3-D printed hollow mold, manufactured ad hoc in a preliminary phase. Then, an optical fiber containing a bare FBG is positioned in the middle of the mold, at the center on the upper surface of the first silicone layer. Once positioned the FBG, the remaining half blend is poured over. An important aspect to be considered is given by the pot life of such silicone rubber, which lasts for a period of 20 min. Indeed, after this time, the silicone starts to cure and harden, becoming tricky to pour. A time interval of 5 h is needed for the silicone curing and, finally, the device is ready and can be removed from the mold.

By implementing this method of fabrication, three sensorized DS patches are developed, having the same dimensions in length L and wide w (i.e., 25 and 5 mm, respectively) and different values of thickness t, as reported in Fig. 2(b).

1) $t_A = 1.3$ mm for patch DS-A.
2) $t_B = 2.5$ mm for patch DS-B.
3) $t_C = 3.5$ mm for patch DS-C.

The hollow molds used to pour the silicone rubber are fabricated by means of the Renkforce RF500 3-D printer, which exploit the fused deposition method. The filament employed for the purpose is in PLA by Renkforce.

III. Results and Discussion

The results of the characterization of the developed sensors in temperature and strain are reported in the following. Then, force tests are performed and detailed, demonstrating the attitude of the devices to measure the force rather than the strain variations.

A. Temperature Characterization

During the thermal tests, the range of environmental thermal variations is investigated. A controlled chamber based on a Peltier cell, shown in Fig. 3(a), is used to heat and cool the sensing devices in the temperature range 5 °C–40 °C. Moreover, the optical instrumentation, consisting in the optical interrogation unit and a PC, is employed to collect the data recorded by the sensors.

The Bragg wavelength shifts recorded by the three devices under test and a bare FBG, used as a temperature reference, are shown in Fig. 3(b) as a function of the temperature.

As reported in Fig. 3(b), all the FBGs embedded in the DS patches show the sensitivity values just slightly higher than the reference sensor, i.e., the bare FBG, with linear behavior and good reversibility. In particular, the temperature sensitivity is 10.5, 11.3, and 12.0 pm·°C^{-1} for DS-A, DS-B, and DS-C, respectively.

Although the thermal expansion coefficient of the silicone rubber of which the patches are made is much higher (i.e., around 250×10^{-6}·°C^{-1}) than that of the silica, which constitutes the optical fiber (i.e., 6×10^{-6}·°C^{-1}), the measured sensitivity values are close to the bare FBG sensitivity, due to the high elasticity of the DS rubber (100% modulus of 22 psi).

Furthermore, comparing the three devices among them, the temperature sensitivity increases with their thickness since the strain contribution, due to the thermal expansion of the patch, increases.

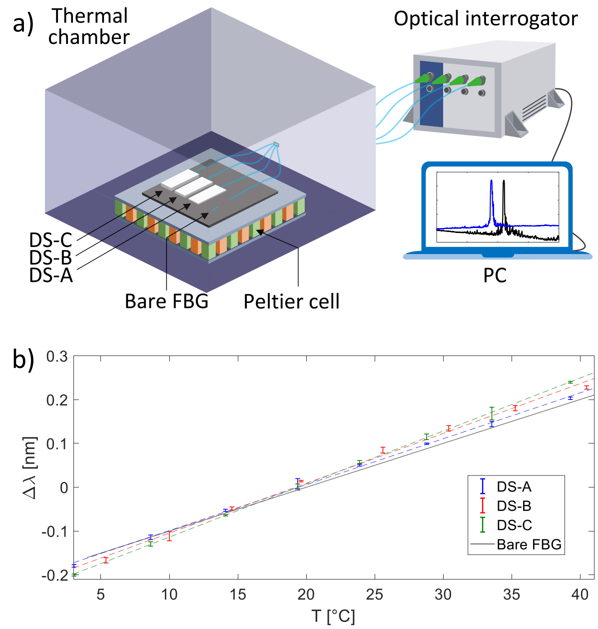

Fig. 3. (a) Schematic of the experimental setup employed for the temperature characterization and (b) results of the performed thermal tests for each of the developed patches in comparison with the trend recorded by the reference sensor, i.e., the bare FBG (the dashed lines represent the straight lines that fit the measuring points minimizing the mean squared error).

B. Strain Characterization

For the characterization in strain, the deformation performances of the DS-embedded FBGs are monitored and the results are reported here. The experimental setup for testing the devices in strain is represented in Fig. 4(a). Beyond the optical instrumentation, it includes a metallic bar, where the DS patches are fixed by means of the silicone adhesive Sil-Poxy by Smooth-On, and different weights to induce the bending in the bar and, thus, strain variations on the sensing devices. In particular, loads up to 6 kg are involved during the test. Therefore, by considering a 1-D structure along the x-axis, having a certain length before bending, a surface strain along the longitudinal direction happens after the structure bending.

In addition to the three devices under test, two bare FBGs are also glued on the bar near to the DS patches to give strain and temperature reference measurements. In particular, the bare FBG used for temperature reference is employed in a strain-free configuration, i.e., it is not glued on the metallic bar, to allow the thermal compensation.

Considering that the FBG sensors are in the middle of the three patches, as shown in Fig. 2, if the DS rubber transmitted all the strain, DS-A, DS-B, and DS-C would be more sensitive than the bare FBG, used as strain reference, since they have a higher distance from the neutral axis of the bar. Moreover, for the same reason, the thickest device, i.e., DS-C, would be the most sensitive. Indeed, according to the beam theory, such strain along the longitudinal direction is proportional to the curvature of the bent structure and, in the hypothesis that the embedding materials transmit the strain, it increases with the distance of the sensor from the neutral axis [27].

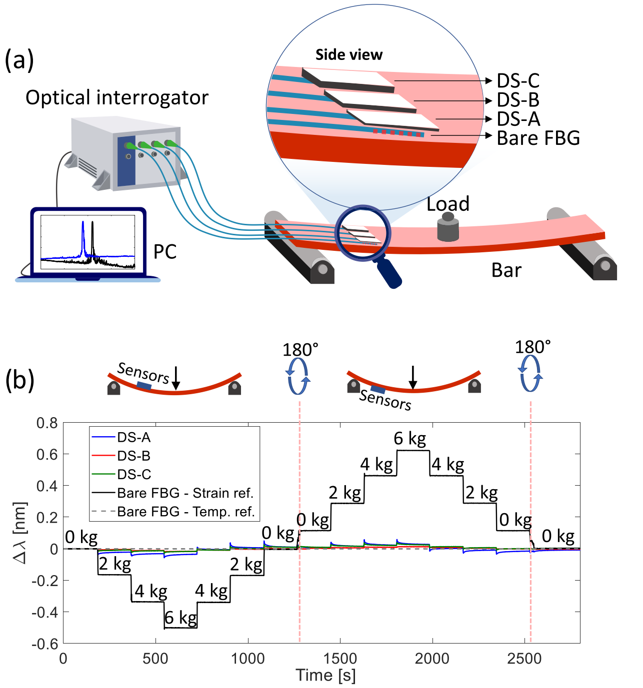

Fig. 4. (a) Schematic of the experimental setup for performing the strain tests and (b) results of the strain characterization recorded by the three DS patches and the two reference FBGs. Strain tests are performed in two configurations, i.e., with FBGs staying on the upper and on the lower side of the metallic bar, as detailed in (b).

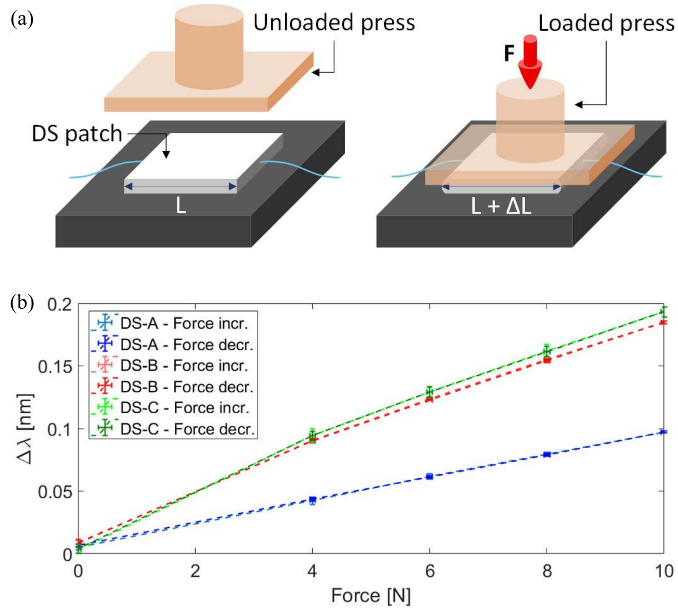

Fig. 5. (a) Schematic of the experimental setup for performing the force tests (a) and (b) results of the force characterization recorded by the three developed DS patches.

Instead, the experimental results reported in Fig. 4(b) show that, differently from what expected by the beam theory, a significant desensitization to strain in the case of the DS patches.

Indeed, the entity of the Bragg wavelength shifts recorded during the test by the DS patches is negligible with respect to the shift measured by the bare FBG. Thus, this leads to conclude that the DS patches do not transmit the strain solicitation from the external surface, touching the metallic bar, to the embedded FBGs due to the high elasticity of silicone rubber.

C. Force Characterization

The last tests concern the investigation of the sensitivity of the DS patches to forces applied perpendicularly to the embedded FBGs. To perform such tests, an appropriate setup, whose schematic is reported in Fig. 5(a), is employed to apply a distributed load on the upper surfaces of the patches. Therefore, each device under test is placed under a little press and loaded with forces up to 10 N, which corresponds to a pressure of 33.3×10^4 Pa considering that the upper surfaces of the patches are of 3 cm^2. Then, data recorded by the FBGs are transmitted to the optical interrogation unit and displayed on the PC, as with the previous tests.

The sensing mechanism is based on the expansion of the rubber in the plane orthogonal to the direction of compression. Indeed, as shown in the loaded press configuration of Fig. 5(a), in correspondence of an applied compressive force F, the length L of the patch is extended by ΔL, depending on the force magnitude.

The results of the force characterization of the three DS patches, collected in Fig. 5(b), demonstrate good linearity and repeatability with absence of hysteresis in the investigated range of forces. A force sensitivity of 9.2, 17.6, and 19.0 pm·N^{-1} for the patches DS-A, DS-B, and DS-C is measured, respectively. It is worth noting that the force sensitivity increases with the patch thickness, even if not linearly. Indeed, as the thickness of the patch increases, its influence on force sensitivity is lower and less relevant.

IV. Conclusion

The FBG-based sensor developed and described here has proved to be an alternative solution to combine force measurements capability with flexibility and wearability. Indeed, besides the advantages introduced by the FBGs, above all electrical safety and small dimensions, by employing an embedding technique in silicone rubber of such sensor, a flexible packaging able to make the FBG sensitive to the force has been obtained.

The silicone-based embedding strategy is implemented and analyzed aiming to develop a systematic study of the sensing capabilities of the FBGs. The device performances, indeed, are assessed as a function of multiple parameters, including environmental factors, i.e., temperature and strain, besides force, and geometrical features of the patch, i.e., its thickness. In particular, three sensors are fabricated, involving different thickness values, i.e., 1.3, 2.5, and 3.5 mm, for patches A, B, and C, respectively, leaving unaltered the other characteristics.

The temperature characterizations results demonstrate a temperature sensitivity ranging from 10.5 to 12.0 pm·°C^{-1}, thus slightly greater with respect to the sensitivity value of the reference sensor (i.e., the bare FBG). Indeed, although the thermal expansion coefficient of the silicone matrix that makes up the patches is more than 40 times higher than the silica one, the very high silicone elasticity dampens this effect, leading to thermal sensitivities close to the one exhibited by the reference FBG. Furthermore, thermal sensitivity can be modulated accordingly with the patch thickness since the thicker is the patch, the higher is the strain contribution acting on the FBG, resulting in a slightly sensitivity increase.

The strain characterization, instead, reveals a strong strain desensitization of the embedded FBGs with respect to the bare one, used as strain reference. The results, indeed, demonstrate very low strain sensitivity, by more than two orders of magnitude with respect to the reference sensor. Therefore, this study demonstrates that silicone embedding insulates the FBGs from the external strain variations.

Finally, the capability of the device to measure the force variations is tested by applying a distributed load on each patch, finding a force sensitivity in the range from 9.2 to 19.0 pm/N, based on the sensor thickness. The experiments, indeed, demonstrate a significative increase of the force sensitivity with the patch thickness, highlighting also that the higher is the thickness, the lower is its influence on the sensitivity.

The reported FBG embedding technique, based on silicone material, allows to provide soft force sensors, which due to their high flexibility and stretchability can be worn and shaped based on the application. Moreover, the proposed study leads to state that the thickness of the developed force sensors affects the temperature, strain, and force sensitivities. Therefore, the developed sensor results in a scalable device, which, depending on its thickness, can improve its sensibility to temperature and force variations and, at the same time, is able to insulate the sensing element from the surrounding strain perturbations.

References

[1] L. Massari et al., "Functional mimicry of Ruffini receptors with fibre Bragg gratings and deep neural networks enables a bio-inspired large-area tactile-sensitive skin," *Nat. Mach. Intell.*, vol. 4, no. 5, pp. 425–435, May 2022.

[2] Q. Liang et al., "Multi-component FBG-based force sensing systems by comparison with other sensing technologies: A review," *IEEE Sensors J.*, vol. 18, no. 18, pp. 7345–7357, Sep. 2018.

[3] M. Amjadi, Y. J. Yoon, and I. Park, "Ultra-stretchable and skin-mountable strain sensors using carbon nanotubes–Ecoflex nanocomposites," *Nanotechnology*, vol. 26, no. 37, Sep. 2015, Art. no. 375501.

[4] M. I. Tiwana, S. J. Redmond, and N. H. Lovell, "A review of tactile sensing technologies with applications in biomedical engineering," *Sens. Actuators A, Phys.*, vol. 179, pp. 17–31, Jun. 2012.

[5] F. Khoshmanesh, P. Thurgood, E. Pirogova, S. Nahavandi, and S. Baratchi, "Wearable sensors: At the frontier of personalised health monitoring, smart prosthetics and assistive technologies," *Biosensors Bioelectron.*, vol. 176, Mar. 2021, Art. no. 112946.

[6] D. Kar, B. George, and K. Sridharan, "A review on flexible sensors for soft robotics," in *Systems for Printed Flexible Sensors*. Bristol, U.K.: IOP Publishing, 2022, pp. 1–15.

[7] P. Di Palma, E. De Vita, A. Iadicicco, and S. Campopiano, "3D shape sensing with FBG-based patch: From the idea to the device," *IEEE Sensors J.*, vol. 22, no. 2, pp. 1338–1345, Jan. 2022.

[8] B. Gholamzadeh and H. Nabovati, "Fiber optic sensors," *Int. J. Electr. Comput. Energ. Electron. Commun. Eng.*, vol. 2, no. 6, pp. 1107–1117, 2008.

[9] D. Hu, S. Lv, Y. Guo, H. He, and J. Liu, "A fiber Bragg grating force sensor with sensitization structure," *IEEE Sensors J.*, vol. 21, no. 3, pp. 3042–3048, Feb. 2020.

[10] H. Song, H. Kim, J. Jeong, and J. Lee, "Development of FBG sensor system for force-feedback in minimally invasive robotic surgery," in *Proc. 5th Int. Conf. Sens. Technol.*, Nov. 2011, pp. 16–20, doi: 10.1109/ICSensT.2011.6136956.

[11] M. S. Müller, L. Hoffmann, T. C. Buck, and A. W. Koch, "Fiber Bragg grating-based force-torque sensor with six degrees of freedom," *Int. J. Optomechtron.*, vol. 3, no. 3, pp. 201–214, Sep. 2009.

[12] C. Lv, S. Wang, and C. Shi, "A high-precision and miniature fiber Bragg grating-based force sensor for tissue palpation during minimally invasive surgery," *Ann. Biomed. Eng.*, vol. 48, no. 2, pp. 669–681, Feb. 2020.

[13] C. Shi, M. Li, C. Lv, J. Li, and S. Wang, "A high-sensitivity fiber Bragg grating-based distal force sensor for laparoscopic surgery," *IEEE Sensors J.*, vol. 20, no. 5, pp. 2467–2475, Mar. 2020.

[14] D. H.-C. Wang, N. Blenman, S. Maunder, V. Patton, and J. Arkwright, "An optical fiber Bragg grating force sensor for monitoring sub-bandage pressure during compression therapy," *Opt. Exp.*, vol. 21, no. 17, p. 19799, Aug. 2013.

[15] A. Leal-Junior et al., "Fiber Bragg gratings in CYTOP fibers embedded in a 3D-printed flexible support for assessment of human–robot interaction forces," *Materials*, vol. 11, no. 11, p. 2305, Nov. 2018.

[16] G. Arnaldo, "Polymer optical fiber strain gauge for human-robot interaction forces assessment on an active knee orthosis," *Opt. Fiber Technol.*, vol. 41, pp. 205–211, Feb. 2018.

[17] A. G. Leal-Junior, C. Marques, M. R. N. Ribeiro, M. J. Pontes, and A. Frizera, "FBG-embedded 3-D printed ABS sensing pads: The impact of infill density on sensitivity and dynamic range in force sensors," *IEEE Sensors J.*, vol. 18, no. 20, pp. 8381–8388, Oct. 2018.

[18] J. Ge, A. E. James, L. Xu, Y. Chen, K.-W. Kwok, and M. P. Fok, "Bidirectional soft silicone curvature sensor based on off-centered embedded fiber Bragg grating," *IEEE Photon. Technol. Lett.*, vol. 28, no. 20, pp. 2237–2240, Jul. 15, 2016.

[19] D. Lo Presti et al., "Wearable system based on flexible FBG for respiratory and cardiac monitoring," *IEEE Sensors J.*, vol. 19, no. 17, pp. 7391–7398, Sep. 2019.

[20] J. Di Tocco et al., "A wearable system based on flexible sensors for unobtrusive respiratory monitoring in occupational settings," *IEEE Sensors J.*, vol. 21, no. 13, pp. 14369–14378, Jul. 2021.

[21] L. Li et al., "Embedded FBG-based sensor for joint movement monitoring," *IEEE Sensors J.*, vol. 21, no. 23, pp. 26793–26798, Dec. 2021.

[22] J. C. Vieira, O. M. F. Morais, C. M. A. Vasques, and R. de Oliveira, "A laboratorial prototype of a weight measuring system using optical fiber Bragg grating sensors embedded in silicone rubber," *Measurement*, vol. 61, pp. 58–66, Feb. 2015.

[23] J.-S. Heo, J.-H. Chung, and J.-J. Lee, "Tactile sensor arrays using fiber Bragg grating sensors," *Sens. Actuators A, Phys.*, vol. 126, no. 2, pp. 312–327, Feb. 2006.

[24] L. Massari, C. M. Oddo, E. Sinibaldi, R. Detry, J. Bowkett, and K. C. Carpenter, "Tactile sensing and control of robotic manipulator integrating fiber Bragg grating strain-sensor," *Frontiers Neurorobotics*, vol. 13, p. 8, Apr. 2019.

[25] E. De Vita et al., "Investigation of the heat sink effect during microwave ablation in hepatic tissue: Experimental and numerical analysis," *IEEE Sensors J.*, vol. 21, no. 20, pp. 22743–22751, Oct. 2021.

[26] D. A. Krohn, T. W. MacDougall, and A. Mendez, *Fiber Optic Sensors: Fundamentals and Applications*. Bellingham, WA, USA: SPIE, 2014.

[27] P. D. Palma, A. Iadicicco, and S. Campopiano, "Curvature sensor based on FBGs embedded in 3D printed patches," *IEEE Sensors J.*, vol. 21, no. 16, pp. 17868–17874, Aug. 2021.

Pasquale Di Palma received the M.Sc. degree in telecommunications engineering from the University of Naples Federico II, Naples, Italy, in 2015, and the Ph.D. degree in information engineering from the University of Naples Parthenope, Naples, in 2019.

Since 2015, he has been with the Department of Engineering, University of Naples Parthenope. His current research interests include the design, simulation, fabrication, and characterization of fiber optic sensors for physical, chemical, and biological applications.

Elena De Vita (Member, IEEE) received the M.Sc. (cum laude) degree in biomedical engineering from the "Università Campus Bio-Medico di Rome," Rome, Italy, in 2018, and the Ph.D. degree in information and communication technology and engineering from the University of Naples "Parthenope," Naples, Italy, in 2022.

She is currently a Postdoctoral Researcher with the Department of Engineering, University of Naples "Parthenope." Her current research interests include fiber optic sensors in biomedical and industrial applications for thermal and mechanical measurements.

Agostino Iadicicco (Member, IEEE) received the master's (cum laude) degree in electronic engineering from the Second University of Naples, Naples, Italy, in 2002, and the Ph.D. degree in information engineering from the University of Sannio, Benevento, Italy, in 2005.

He is currently a Professor with the Department of Engineering, University of Naples Parthenope, Naples. Since 2002, his research activity has been focused on optoelectronics and photonics devices for sensing and communications applications. He is currently involved in the design, realization, and testing of novel in-fiber devices in standard and unconventional fibers including polarization maintaining and photonic bandgap fibers. His work in this area encompasses the development and practical application of sensors for the measurement of a range of physical, chemical, and biological parameters.

Dr. Iadicicco is a member of the Ph.D. Teaching Council and serves as an Associate Editor for the IEEE SENSORS JOURNAL.

Stefania Campopiano (Member, IEEE) received the master's (cum laude) degree in electronic engineering from the University of Naples Federico II, Naples, Italy, and the Ph.D. degree in electronic engineering from Università della Campania L. Vanvitelli, Caserta, Italy.

She is currently a Full Professor of Electronics and Optoelectronics with the University of Naples Parthenope, Naples, where she coordinates the information engineering study course. She is a Ph.D. Teaching Staff Member. She is a Tutor of several Ph.D. students. Her main research field is in the area of optoelectronic sensors and devices. She has authored over 200 printed works, including international journals and conferences, and coauthored patents. Her current research interests include nondestructive characterization of semiconductor and dielectric materials, integrated optic sensors, and fiber optic and fiber Bragg grating (FBG)-based sensors systems. She cooperates on scientific arguments with several universities and companies in Italy and abroad.

Dr. Campopiano is a Reviewer of IEEE, OSA, and Elsevier journals.

Open Access funding provided by 'Università degli Studi di Napoli "Parthenope"' within the CRUI CARE Agreement